Unconsciousness reconfigures modular brain network dynamics

Sofía Morena del Pozo - sofiamorenadelpozo@gmail.com

PhD. advisors and co-authors: Pablo Balenzuela & Enzo Tagliazucchi

7-10 February 2023,
Buenos Aires, Argentina.

SoPhy Lab http://sophy.df.uba.ar
COCUCO Lab https://www.cocucolab.org

Universidad de Buenos Aires - Exactas
departamento de física

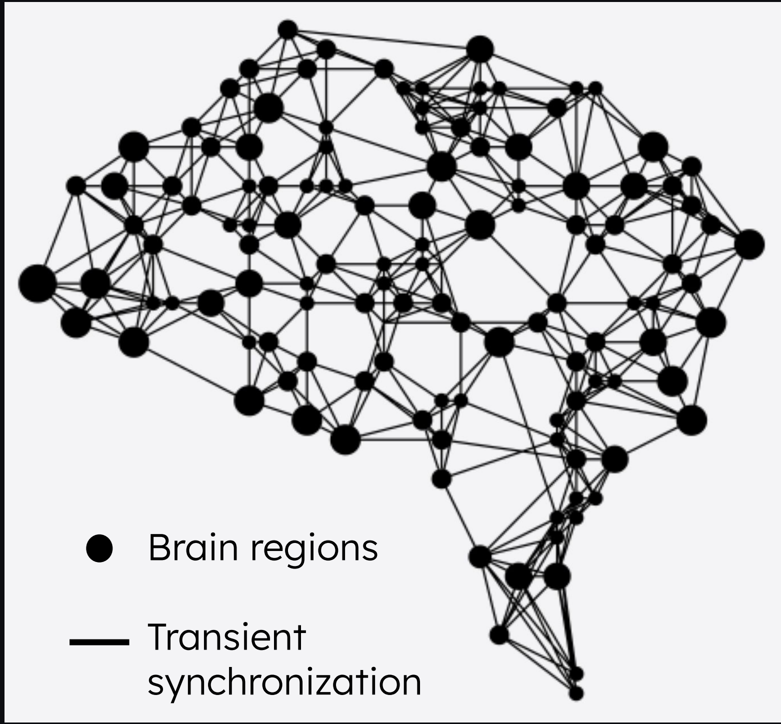
Brain regions
Transient synchronization

What should be the **modular structure** of a dynamic **brain network** of a **conscious** person?

The dynamic core hypothesis

Conscious experience <-> Neural processes in the human brain

*Edelman, Gerald M and Tononi, Giulio. *Reentry and the dynamic core: neural correlates of conscious experience*. Press Cambridge, Neural correlates of consciousness: Empirical and conceptual questions, 139 (2000).

The dynamic core hypothesis

Conscious experience <-> Neural processes in the human brain

“Consciousness is correlated with simultaneously integrated and differentiated assemblies of transiently synchronized brain regions.”

*Edelman, Gerald M and Tononi, Giulio. *Reentry and the dynamic core: neural correlates of conscious experience*. Press Cambridge, Neural correlates of consciousness: Empirical and conceptual questions, 139 (2000).

The dynamic core hypothesis

Conscious experience <-> Neural processes in the human brain

“Consciousness is correlated with simultaneously integrated and differentiated assemblies of transiently synchronized brain regions.”

Dynamic core -> Large number of possible configurations.

*Edelman, Gerald M and Tononi, Giulio. *Reentry and the dynamic core: neural correlates of conscious experience*. Press Cambridge, Neural correlates of consciousness: Empirical and conceptual questions, 139 (2000).

The dynamic core hypothesis

Conscious experience <-> Neural processes in the human brain

"Consciousness is correlated with simultaneously integrated and differentiated assemblies of transiently synchronized brain regions."

Dynamic core -> Large number of possible configurations.

Constrained to represent highly integrated brain states

*Edelman, Gerald M and Tononi, Giulio. *Reentry and the dynamic core: neural correlates of conscious experience*. Press Cambridge, Neural correlates of consciousness: Empirical and conceptual questions, 139 (2000).

<u>The dynamic core hypothesis</u>

Conscious experience <-> Neural processes in the human brain

"Consciousness is correlated with simultaneously integrated and differentiated assemblies of transiently synchronized brain regions."

Dynamic core -> Large number of possible <u>configurations</u>.

↓

Constrained to represent highly integrated brain states

The dynamic core consists of a sequence exploring an ample repertoire of highly integrated brain states.

*Edelman, Gerald M and Tononi, Giulio. *Reentry and the dynamic core: neural correlates of conscious experience*. Press Cambridge, Neural correlates of consciousness: Empirical and conceptual questions, 139 (2000).

The dynamic core hypothesis

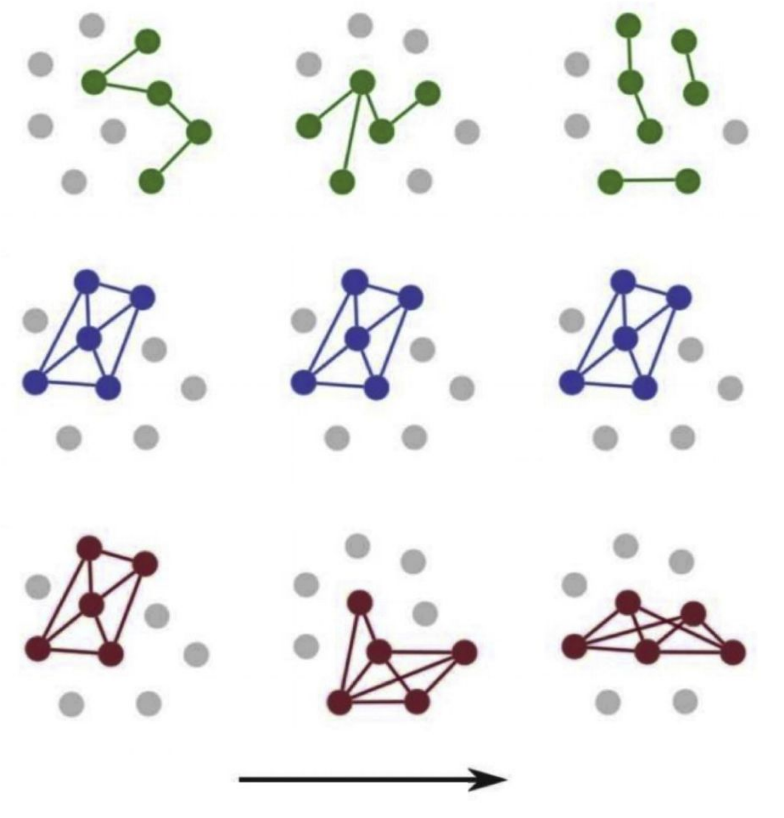

The dynamic core hypothesis

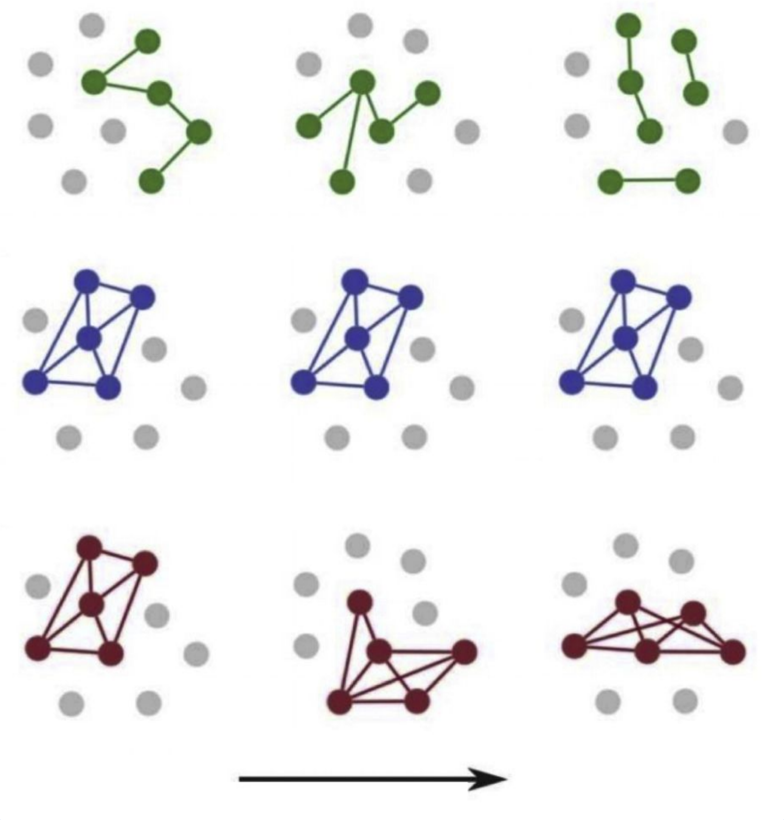

 Differentiated but  integrated (segregated) states.

The dynamic core hypothesis

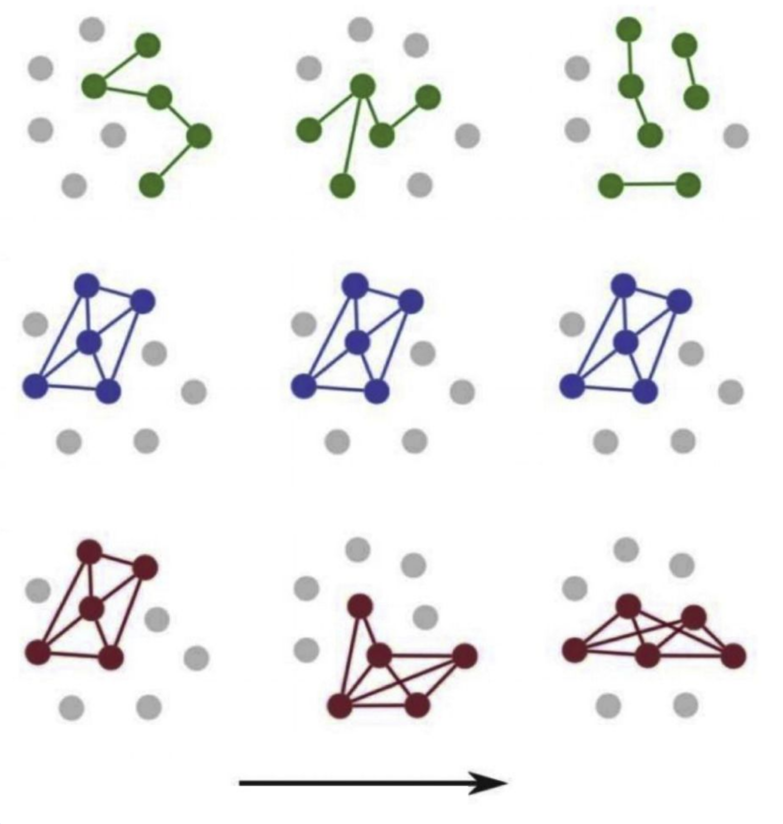

Differentiated but integrated (segregated) states.

Differentiated but integrated states.

The dynamic core hypothesis

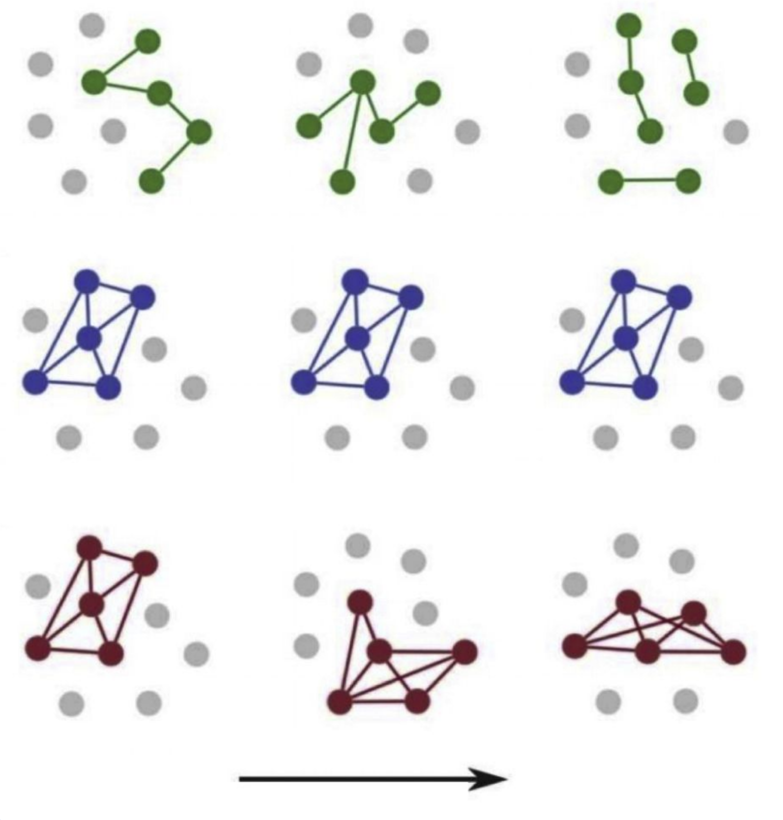

Differentiated but integrated (segregated) states.

Differentiated but integrated states.

Different configuration integrated dynamic core.

The dynamic core hypothesis

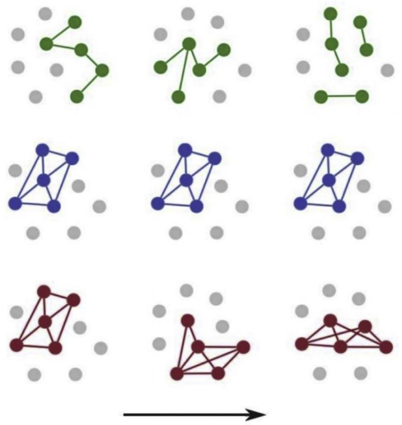

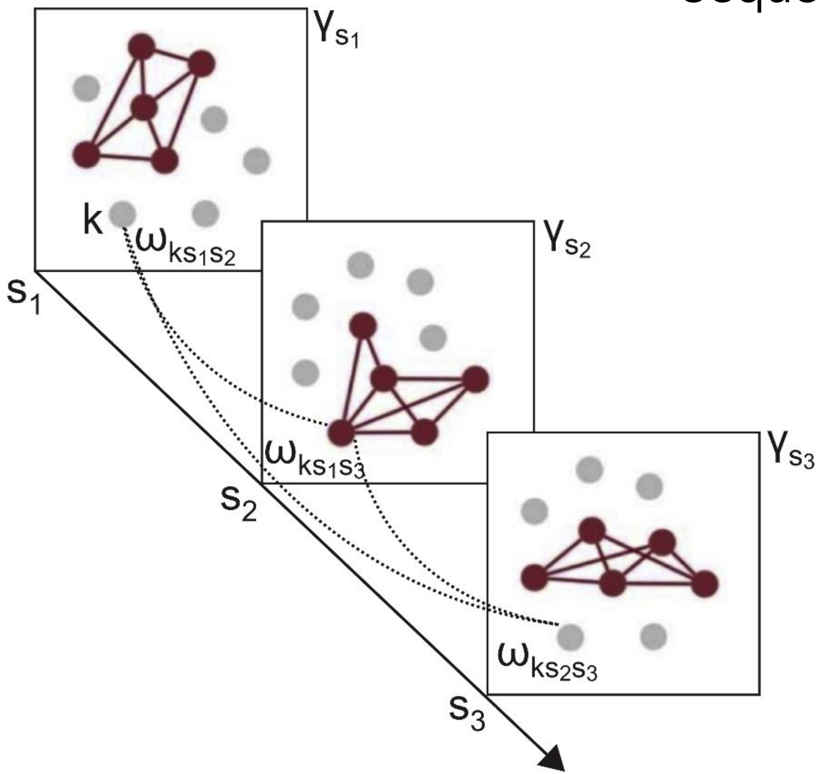

Sequence of brain states

Multilayer network

The dynamic core hypothesis

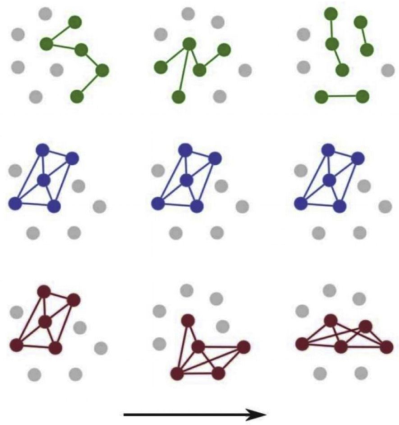

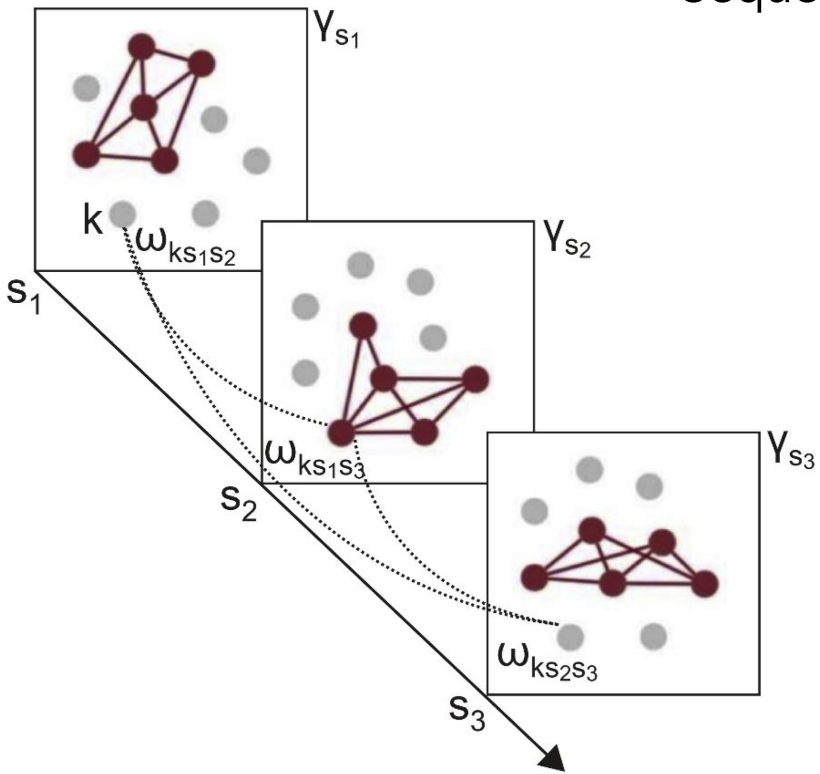

Sequence of brain states

Multilayer network

DYNAMIC CORE

Time-dependent community.

Despite previous research, the **relationship** between **consciousness** and the **modular structure** of multilayer **brain networks** remains to be investigated.

What did we do?

1. We constructed **multilayer connectivity networks** from **fMRI** recordings acquired **during states of reduced consciousness**: under propofol anesthesia and deep sleep.

* For more details see https://doi.org/10.1063/5.0046047
** P. J. Mucha, T. Richardson, K. Macon, M. A. Porter, and J.-P. Onnela, Community structure in time-dependent, multiscale, and multiplex networks, science 328, 876 (2010).

What did we do?

1. We constructed **multilayer connectivity networks** from **fMRI** recordings acquired **during states of reduced consciousness**: under propofol anesthesia and deep sleep.

Sequence of brain states:

↓

Multilayer network

↓

DYNAMIC CORE

↕

Time-dependent community.

I. **Propofol**-induced loss of consciousness**:** 18 volunteers were scanned with fMRI during wakefulness (**W**), propofol sedation (**S**), propofol-induced loss of consciousness (**LOC**).

II. Human NREM **sleep:** fMRI data from 63 subjects acquired during wakefulness (**W**), 27 during **N1** sleep, 33 during **N2** sleep and 17 during **N3** sleep* .

* For more details see https://doi.org/10.1063/5.0046047

** P. J. Mucha, T. Richardson, K. Macon, M. A. Porter, and J.-P. Onnela, Community structure in time-dependent, multiscale, and multiplex networks, science 328, 876 (2010).

What did we do?

1. We constructed **multilayer connectivity networks** from **fMRI** recordings acquired **during states of reduced consciousness**: under propofol anesthesia and deep sleep.

Sequence of brain states:

Multilayer network

DYNAMIC CORE

Time-dependent community.

I. **Propofol-induced loss of consciousness:** 18 volunteers were scanned with fMRI during wakefulness (**W**), propofol sedation (**S**), propofol-induced loss of consciousness (**LOC**).

II. Human NREM **sleep:** fMRI data from 63 subjects acquired during wakefulness (**W**), 27 during **N1** sleep, 33 during **N2** sleep and 17 during **N3** sleep* .

Time-dependent community detection → Using the ***multilayer Louvain algorithm*** **

* For more details see https://doi.org/10.1063/5.0046047

** P. J. Mucha, T. Richardson, K. Macon, M. A. Porter, and J.-P. Onnela, Community structure in time-dependent, multiscale, and multiplex networks, science 328, 876 (2010).

What did we do?

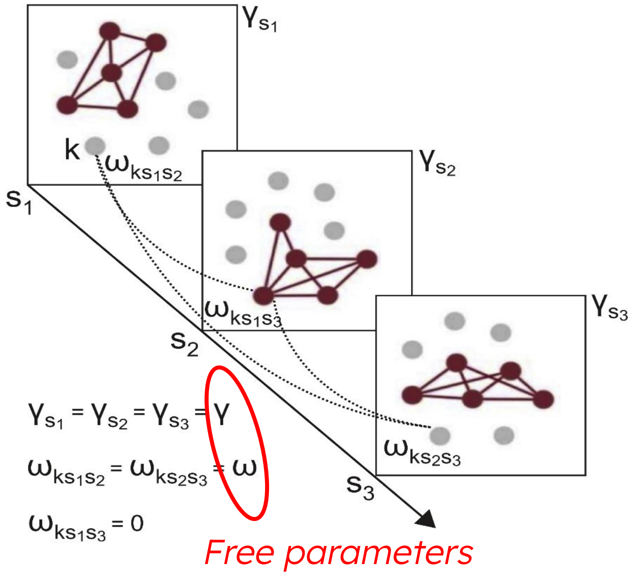

ω -> Connectivity strength between temporal layers

ɣ -> Characteristic size of the detected modules

* For more details see https://doi.org/10.1063/5.0046047

** P. J. Mucha, T. Richardson, K. Macon, M. A. Porter, and J.-P. Onnela, Community structure in time-dependent, multiscale, and multiplex networks, science 328, 876 (2010).

What did we do?

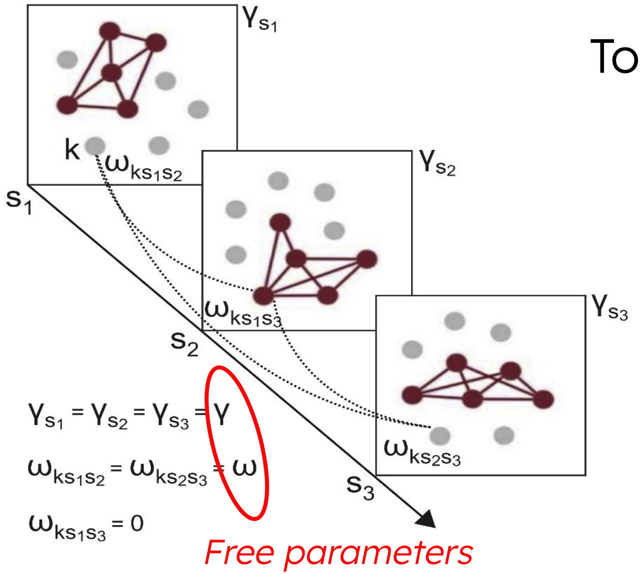

To find the **optimal parameters** of this algorithm:

We developed a **benchmark** for module detection in heterogeneous temporal networks.

ω -> Connectivity strength between temporal layers

ɣ -> Characteristic size of the detected modules

* For more details see https://doi.org/10.1063/5.0046047

** P. J. Mucha, T. Richardson, K. Macon, M. A. Porter, and J.-P. Onnela, Community structure in time-dependent, multiscale, and multiplex networks, science 328, 876 (2010).

<u>Benchmark for time-dependent module detection</u>

- *<u>Static benchmark</u>* * :
  - Scale-free degree distributions
  - Scale-free module size distributions.

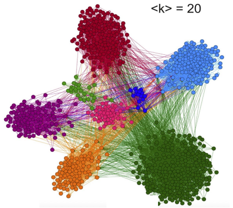

* A. Lancichinetti, S. Fortunato, and F. Radicchi, Benchmark graphs for testing community detection algorithms, Physical review E 78, 046110 (2008).
** C. Granell, R. K. Darst, A. Arenas, S. Fortunato, and S. G omez, Benchmark model to assess community structure in evolving networks, Physical Review E 92, 012805 (2015).
*** For more details about the benchmark see https://doi.org/10.1063/5.0046047.

Benchmark for time-dependent module detection

- *Static benchmark* * :
  - Scale-free degree distributions
  - Scale-free module size distributions.

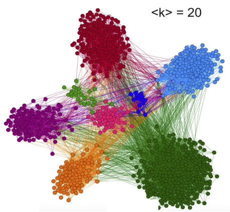

- *Temporal evolution* on this based on two different dynamic processes**:
  - Division of communities.
  - Contraction of communities.

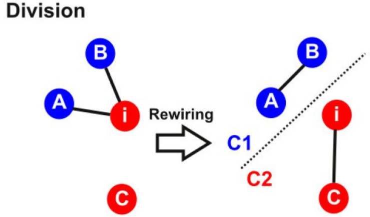

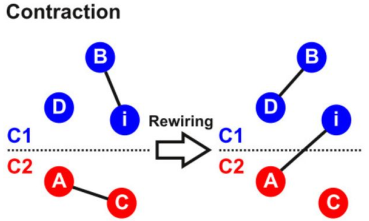

* A. Lancichinetti, S. Fortunato, and F. Radicchi, Benchmark graphs for testing community detection algorithms, Physical review E 78, 046110 (2008).
** C. Granell, R. K. Darst, A. Arenas, S. Fortunato, and S. G omez, Benchmark model to assess community structure in evolving networks, Physical Review E 92, 012805 (2015).
*** For more details about the benchmark see https://doi.org/10.1063/5.0046047.

Benchmark for time-dependent module detection

- *Static benchmark* * :
  - Scale-free degree distributions
  - Scale-free module size distributions.

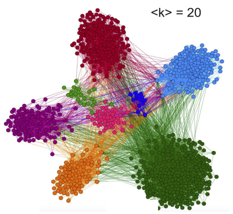

- *Temporal evolution* on this based on two different dynamic processes**:
  - Division of communities.
  - Contraction of communities.

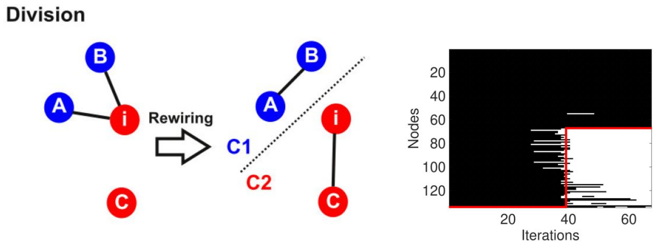

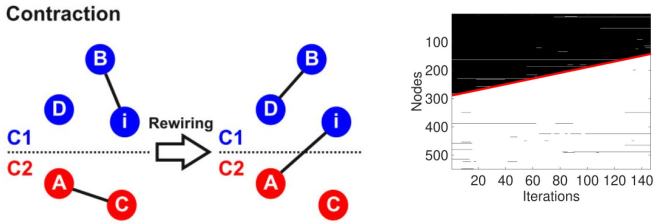

* A. Lancichinetti, S. Fortunato, and F. Radicchi, Benchmark graphs for testing community detection algorithms, Physical review E 78, 046110 (2008).
** C. Granell, R. K. Darst, A. Arenas, S. Fortunato, and S. G omez, Benchmark model to assess community structure in evolving networks, Physical Review E 92, 012805 (2015).
*** For more details about the benchmark see https://doi.org/10.1063/5.0046047.

Benchmark for time-dependent module detection

- *Static benchmark* * :
  - Scale-free degree distributions
  - Scale-free module size distributions.

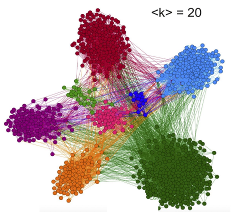

Optimal parameters
γ= 0.55** and **ω = 1

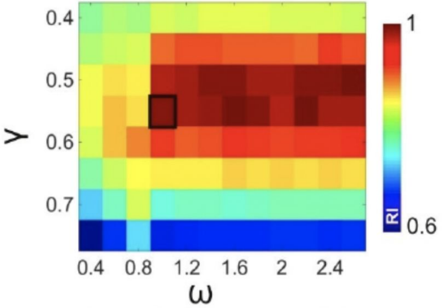

- *Temporal evolution* on this based on two different dynamic processes**:
  - Division of communities.
  - Contraction of communities.

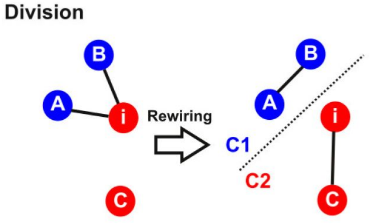

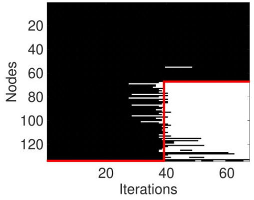

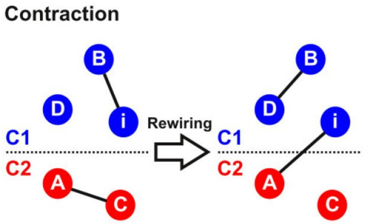

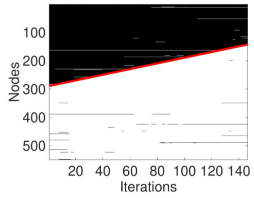

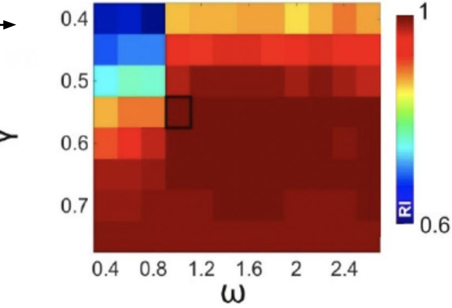

* A. Lancichinetti, S. Fortunato, and F. Radicchi, Benchmark graphs for testing community detection algorithms, Physical review E 78, 046110 (2008).
** C. Granell, R. K. Darst, A. Arenas, S. Fortunato, and S. G omez, Benchmark model to assess community structure in evolving networks, Physical Review E 92, 012805 (2015).
*** For more details about the benchmark see https://doi.org/10.1063/5.0046047.

Results

We obtained the **time-dependent modular structure of fMRI functional connectivity networks**

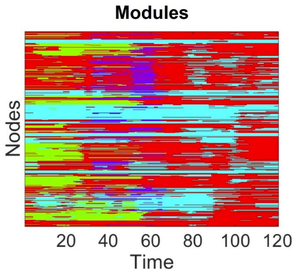

Results

We obtained the **time-dependent modular structure of fMRI functional connectivity networks**

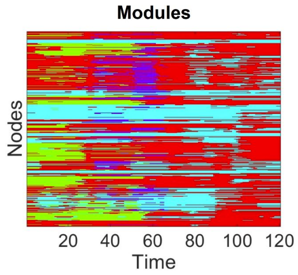

We focused on two metrics related to the dynamics of communities :

Results

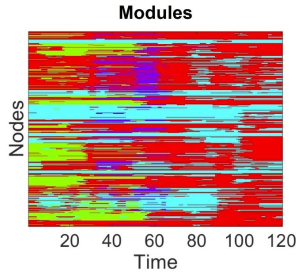

We obtained the **time-dependent modular structure of fMRI functional connectivity networks**

We focused on two metrics related to the dynamics of communities :

- **Largest multilayer module (LMM)** -identified with **dynamic core**-

$$LMM = \frac{\max_i |G_{it}|}{NT}$$

(fraction of nodes in biggest module)

Results

We obtained the **time-dependent modular structure of fMRI functional connectivity networks**

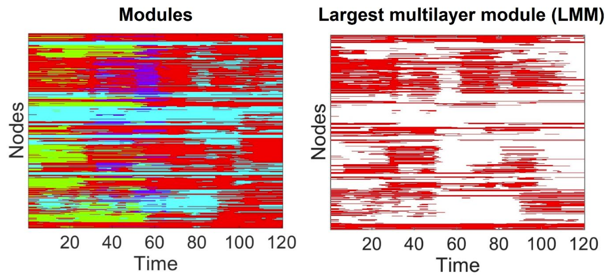

We focused on two metrics related to the dynamics of communities :

- **Largest multilayer module (LMM)** -identified with **dynamic core**-

$$LMM = \frac{\max_i |G_{it}|}{NT}$$

(fraction of nodes in biggest module)

Results

We obtained the **time-dependent modular structure of fMRI functional connectivity networks**

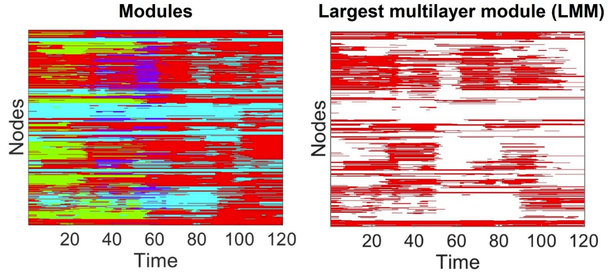

We focused on two metrics related to the dynamics of communities :

- **Largest multilayer module (LMM)** -identified with **dynamic core**-

$$LMM = \frac{\max_i |G_{it}|}{NT}$$

(fraction of nodes in biggest module)

- **Flexibility**, which we interpreted as the degree of **differentiation of the dynamic core**.

$$F_i = \frac{|\{t : M_{it} \neq M_{it+1}\}|}{T}$$

(rate of alternation)

- **Flexibility** $$F_i = \frac{|\{t : M_{it} \neq M_{it+1}\}|}{T}$$ *(rate of alternation)*

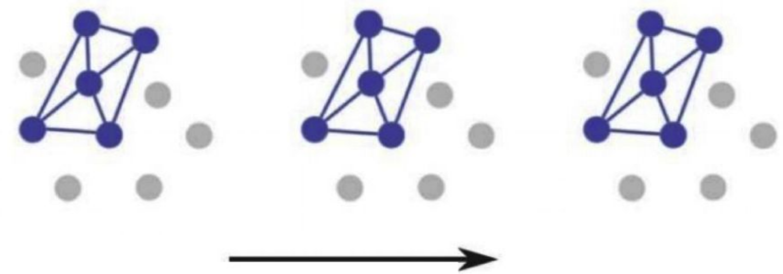

$$\longrightarrow F_i = 0 \; \forall \; i$$

- **Largest multilayer module (LMM)**

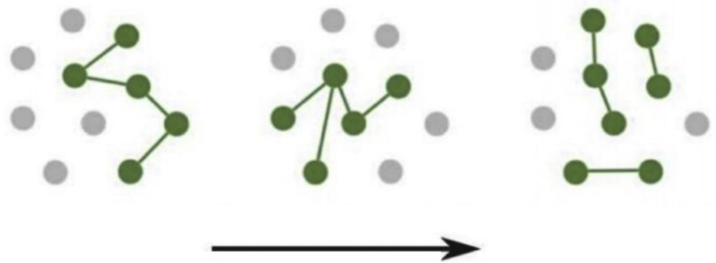

$<$

LMM

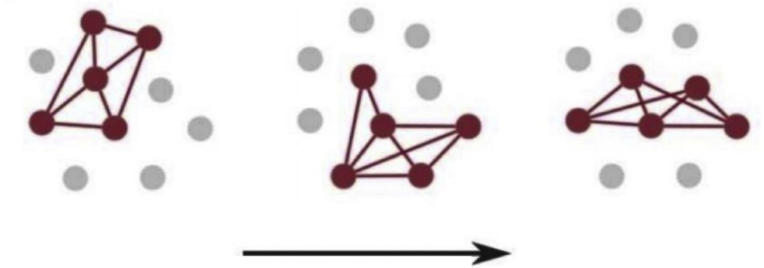

Results

Flexibility (LMM) during Wake vs. sleep stages

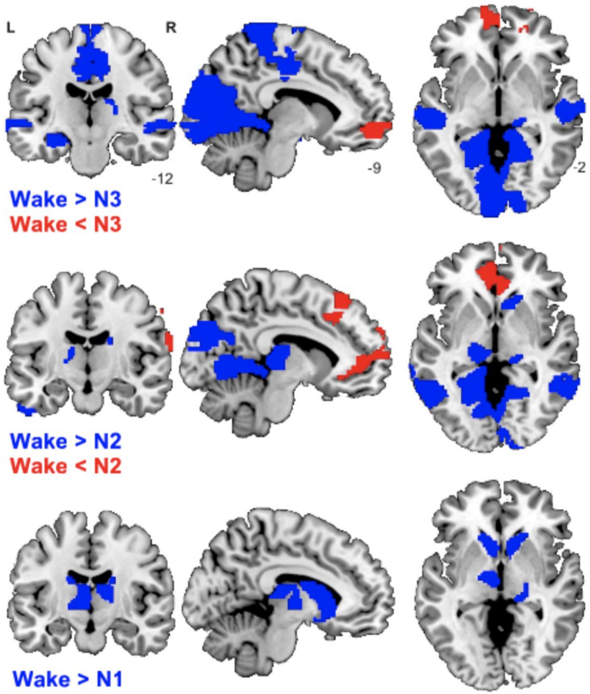

Decreased flexibility during sleep

Increased flexibility during sleep

Results

Flexibility (LMM) during Wake vs. sleep stages

Majority of nodes **decreased their flexibility during sleep** -> In regions related to sensory perception.

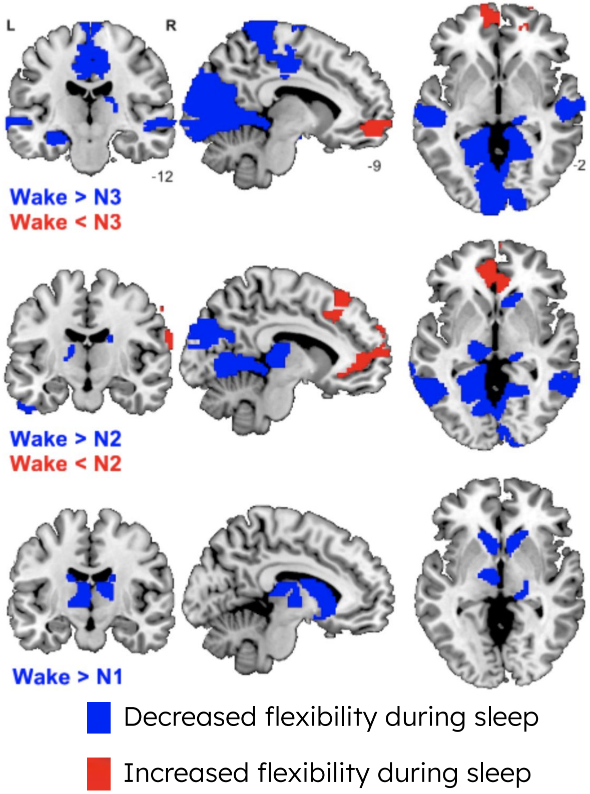

Results

Flexibility (LMM) during Wake vs. sleep stages

Majority of nodes **decreased their flexibility during sleep** -> In regions related to sensory perception. In particular, flexibility decreases during N1 sleep were observed mostly for thalamic nodes, consistent with the observation that the **thalamus** becomes deactivated and disconnected from sensory cortices during early sleep.

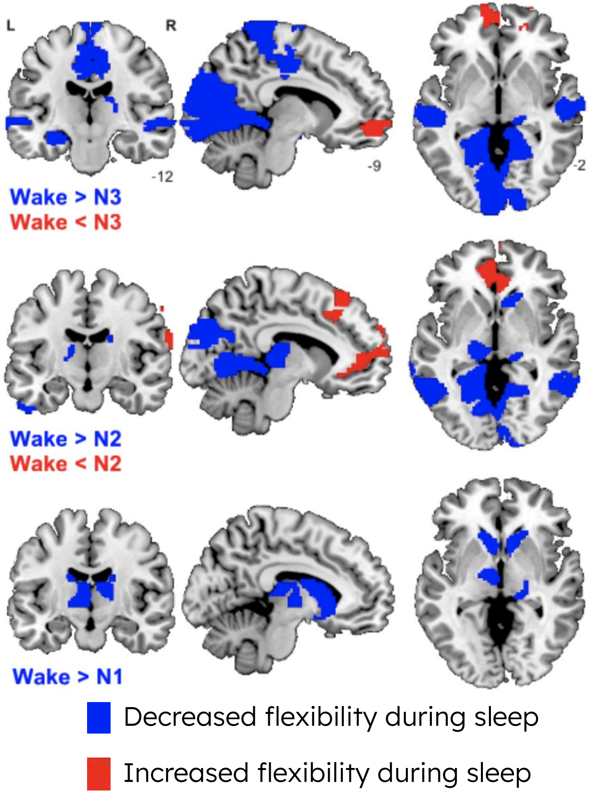

Results

Flexibility (LMM) during Wake vs. sleep stages

Majority of nodes **decreased their flexibility during sleep** -> In regions related to sensory perception. In particular, flexibility decreases during N1 sleep were observed mostly for thalamic nodes, consistent with the observation that the **thalamus** becomes deactivated and disconnected from sensory cortices during early sleep.

Conversely, flexibility increased during sleep only in **frontal regions** associated with higher cognitive functions, with the strongest increases seen during N3 sleep.

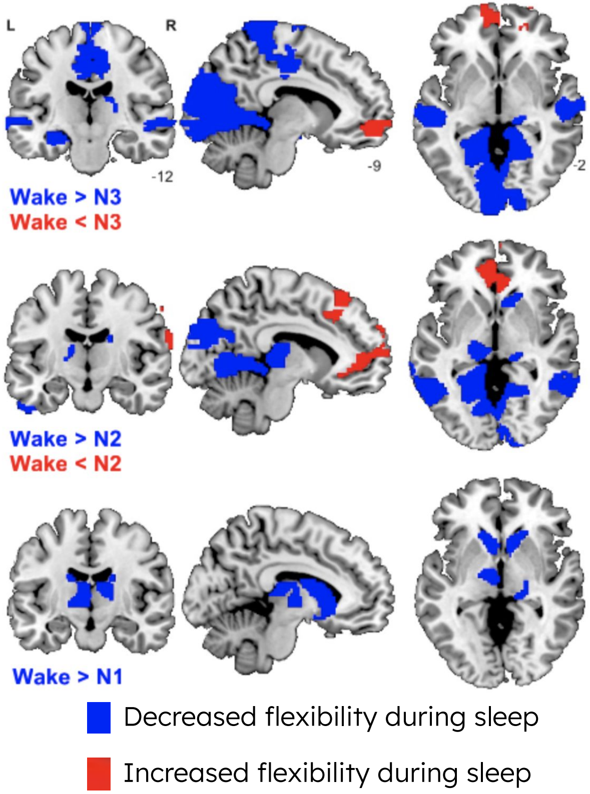

Results

A: Significant differences in the regional **probability of belonging to the largest multilayer module (LMM)** for wakefulness vs. N3 sleep (left) and vs. LOC.

While changes were more widespread and significant during N3 sleep, LOC was also associated with decreases in sensorimotor regions, and increases in frontal regions

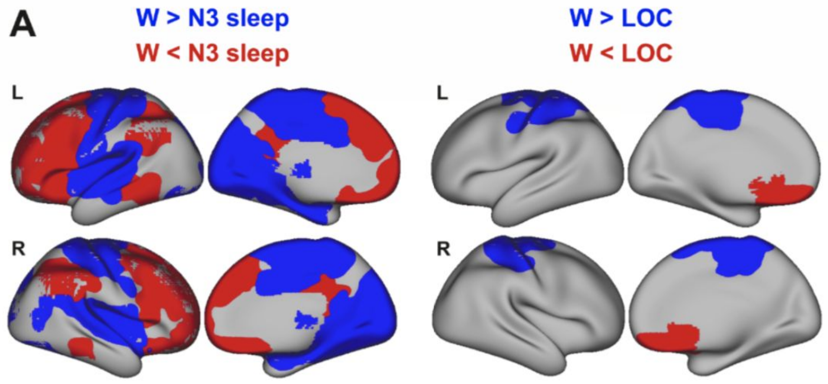

Results

A: Significant differences in the regional **probability of belonging to the largest multilayer module (LMM)** for wakefulness vs. N3 sleep (left) and vs. LOC.

While changes were more widespread and significant during N3 sleep, LOC was also associated with decreases in sensorimotor regions, and increases in frontal regions

B: A Scatter plot of the change in the probability of belonging to the LMM for N3 vs. LOC, it shows a **similar spatial pattern of changes.**

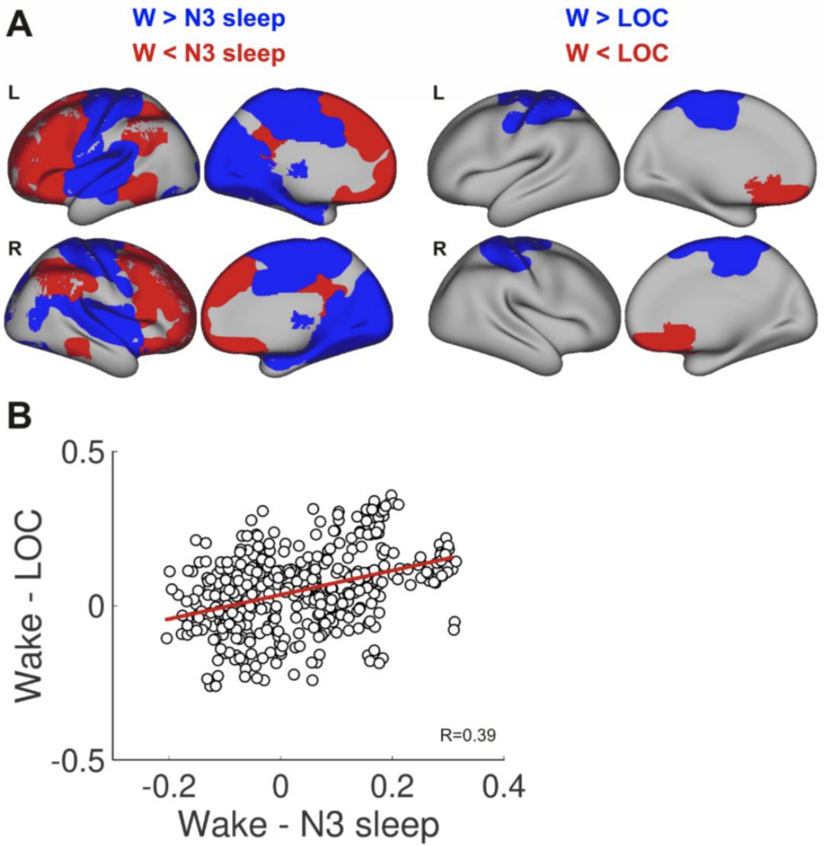

Results

A: Significant differences in the regional **probability of belonging to the largest multilayer module (LMM)** for wakefulness vs. N3 sleep (left) and vs. LOC.

While changes were more widespread and significant during N3 sleep, LOC was also associated with decreases in sensorimotor regions, and increases in frontal regions

B: A Scatter plot of the change in the probability of belonging to the LMM for N3 vs. LOC, it shows a **similar spatial pattern of changes.**

C: Boxplots for the normalized size of the largest multilayer module. In both cases (N3 sleep and LOC), the **LMM decreased in size** during loss of consciousness.

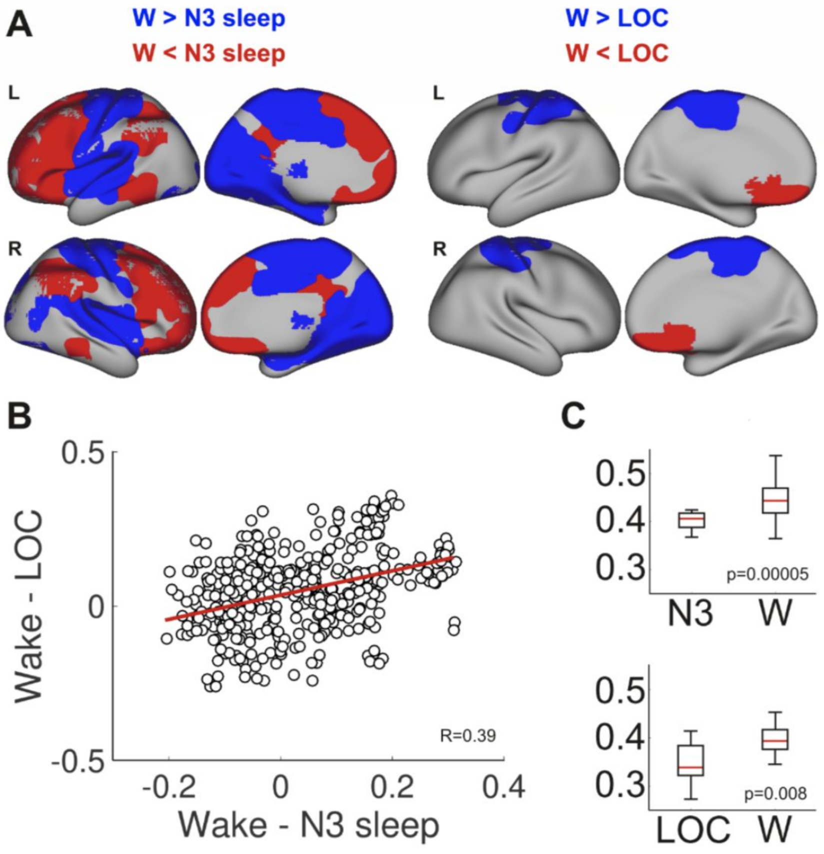

Conclusions

- **Systematic framework** to evaluate the performance of modularity optimization algorithms.

Conclusions

- **Systematic framework** to evaluate the performance of modularity optimization algorithms.
- We found converging evidence of a **reconfiguration of the largest multilayer module** during deep sleep and general anesthesia:

Conclusions

- **Systematic framework** to evaluate the performance of modularity optimization algorithms.
- We found converging evidence of a **reconfiguration of the largest multilayer module** during deep sleep and general anesthesia:
  - **Size of LMM** was reduced during deep sleep and general anesthesia -> Supports the hypothesis that consciousness can vanish as a consequence of fragmented dynamic core.

Conclusions

- **Systematic framework** to evaluate the performance of modularity optimization algorithms.
- We found converging evidence of a **reconfiguration of the largest multilayer module** during deep sleep and general anesthesia:
    - **Size of LMM** was reduced during deep sleep and general anesthesia -> Supports the hypothesis that consciousness can vanish as a consequence of fragmented dynamic core.
    - The **regional correlation** of the changes in the **probability of belonging to the LLM** during deep sleep and anesthesia suggests that this metric could capture a signature of loss of consciousness present in both conditions.

Conclusions

- **Systematic framework** to evaluate the performance of modularity optimization algorithms.
- We found converging evidence of a **reconfiguration of the largest multilayer module** during deep sleep and general anesthesia:
    - **Size of LMM** was reduced during deep sleep and general anesthesia -> Supports the hypothesis that consciousness can vanish as a consequence of fragmented dynamic core.
    - The **regional correlation** of the changes in the **probability of belonging to the LLM** during deep sleep and anesthesia suggests that this metric could capture a signature of loss of consciousness present in both conditions.
    - **Flexibility** decreased during sleep: Majority of the regions decreased their rate of alternation between the LMM and the rest of the modules, paralleling the consolidation of deeper sleep stages.

Conclusions

- **Systematic framework** to evaluate the performance of modularity optimization algorithms.
- We found converging evidence of a **reconfiguration of the largest multilayer module** during deep sleep and general anesthesia:
    - **Size of LMM** was reduced during deep sleep and general anesthesia -> Supports the hypothesis that consciousness can vanish as a consequence of fragmented dynamic core.
    - The **regional correlation** of the changes in the **probability of belonging to the LLM** during deep sleep and anesthesia suggests that this metric could capture a signature of loss of consciousness present in both conditions.
    - **Flexibility** decreased during sleep: Majority of the regions decreased their rate of alternation between the LMM and the rest of the modules, paralleling the consolidation of deeper sleep stages.
- Future studies should assess whole-brain dynamics simultaneously with **different methods** to understand whether the dynamic core fluctuates over **scales inaccessible to fMRI**, and whether these fluctuations are manifest at the behavioral and cognitive levels.

Thank you!

Chaos
An Interdisciplinary Journal of Nonlinear Science

Unconsciousness reconfigures modular brain network dynamics

Cite as: Chaos **31**, 093117 (2021); https://doi.org/10.1063/5.0046047
Submitted: 31 January 2021 • Accepted: 04 August 2021 • Published Online: 21 September 2021

Sofía Morena del Pozo, Helmut Laufs, Vincent Bonhomme, et al.

COLLECTIONS

F This paper was selected as Featured

Pablo Balenzuela

Me

Enzo Tagliazucchi

Thank you!

Appendix

fMRI time series and communities

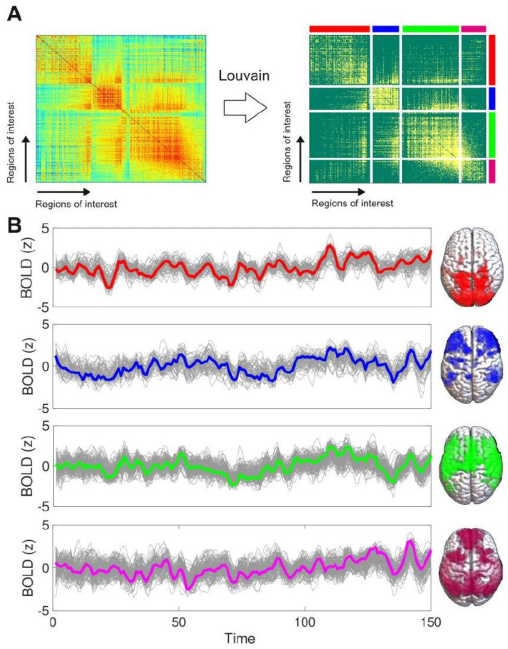

Figure S1. A) Example functional connectivity matrix before (left) and after (right) thresholding. The right panel shows the modular structure of the network, obtained using the Louvain algorithm. B) Example time series associated with different functional modules. Grey lines represent time series from each individual ROI in the module and colored lines indicate the mean time series. The anatomical distributions of the modules are shown on the right.

Time-dependent benchmark algorithm

Null model based on division of communities: Division

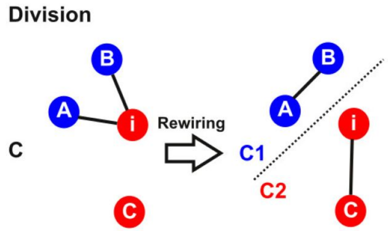

We start from a network with N nodes and apply the following steps:

1. A module named C, sufficiently large for the division into smaller sub-modules, is chosen at random.
2. The nodes belonging to C are assigned to two sub-modules, C1 and C2. A fraction x of the nodes in C belongs to C1, and $(1-x)$ belongs to C2.
3. For each node i in C2, we apply the following steps:
   (a) μ_{21i} of node i is calculated as:
   $\mu_{21i} = \frac{\#\text{Links with C1 nodes}}{\#\text{Total links}}$
   (b) A mixing parameter between communities is chosen per node, μ_{12}.
   (c) While $\mu_{21i} > \mu_{12}$ nodes a, b and c are searched such that they meet the conditions set forth in the division step presented in the rewiring scheme: node a and node b belong to C1 and are connected to node i, node c belongs to C2 and is not connected to node i.
   (d) The link between node i and node b is deleted and a new link is created connecting it to node a. This is repeated until there are no more nodes a, b and c meeting these conditions or until $\mu_{21i} < \mu_{12}$. The rewiring scheme is presented in the rewiring scheme.
   (e) The final adjacency sub-matrix is saved as the dynamic network at time $t = i$.

*The combination of these two processes allowed us to represent the most frequent behaviours seen in the dynamics of brain real modular systems ****

Time-dependent benchmark algorithm

Null model based on expansion-contraction of communities: Contraction

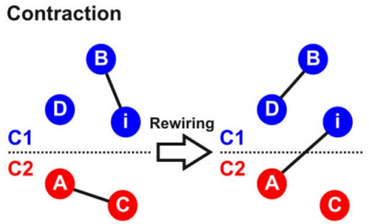

It is an algorithm that selects two random modules from a certain complex network with N nodes, and then grows the size of one module at the expense of the other. The steps are as follows:

1. Two modules C1 and C2 are chosen at random.
2. The adjacency matrix is reordered so that the two modules appear consecutively. The adjacency sub-matrix containing modules C1 and C2 is selected.
3. C1 nodes are re-tagged and rewired, changing their membership to C2: Let n_1 be the number of C1 nodes, ranging from 1 to the $X-th$ node of C1, where X is the integer part of $n_1 x$. The following steps are applied to each node i of this set:
   (a) μ_{12i} of node i is calculated as,
   $\mu_{12i} = \frac{\#\text{Links with C2 nodes}}{\#\text{Total links}}$
   (b) A mixing parameter between modules is chosen per node, μ_{12}
   (c) While $\mu_{12i} > \mu_{12}$, nodes a, b, c and d are searched such that they meet the conditions set forth in the rewiring scheme.
   (d) The link from node i to node b is deleted, and a new link is created between node i and node a. This is repeated until there are no more nodes a and b fulfilling these conditions, or until $\mu_{12i} < \mu_{12}$.
   (e) Node i is removed from C1 and added to C2.
   (f) The average degree of intercommunity links of C2 nodes ($< k_{iC2} >$) and the degree of node i (k_i) are calculated.
   (g) While $k_i << k_{iC2} >$ pairs of nodes whose C2 intramodular degrees are between $< k_{iC2} >$ and k_{max} are selected. The links between those nodes are deleted, and new links between node i and other nodes in C2 with $k << k_{iC2} >$ are added.
   (h) The final adjacency sub-matrix is saved as the dynamic network at time $t = i$.

Time-dependent benchmark algorithm

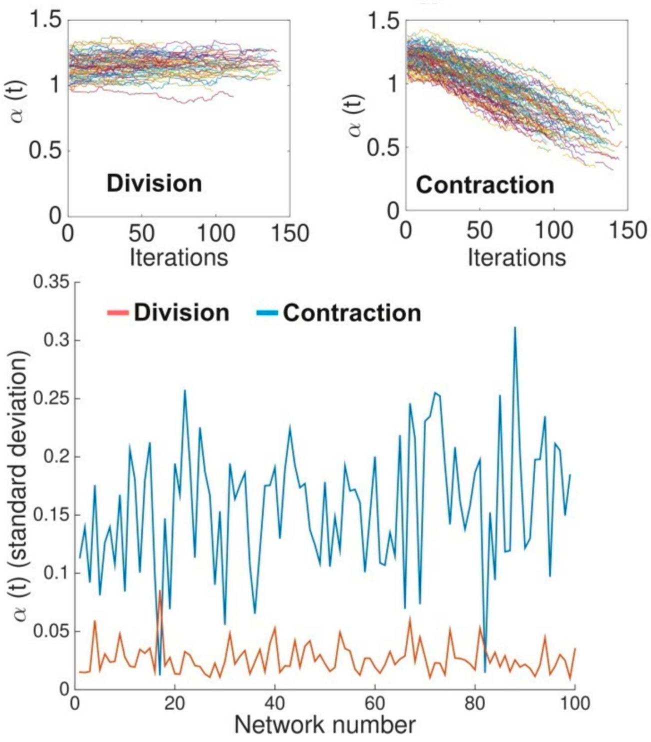

The coefficient of the power law for the degree distribution, α(t), and the standard deviation of for both dynamics vs time.

Louvain method for community detection implemented in MATLAB

We consider a multilayer network with adjacency matrix given by A_{ijs}, where i and j index the network node and s indexes the layer, which is here interpreted as a temporal dimension. Given a certain partition, its multilayer modularity (Q) is computed as

$$Q = \frac{1}{2\mu} \sum_{ijrs} \left[\left(A_{ijs} - \gamma_s \frac{k_{is} k_{js}}{2m_s} \delta_{sr} \right) + \delta_{ij} \omega_{jsr} \right] \delta(g_{is}, g_{jr}),$$

where $k_{js} = \sum_i A_{ijs}$, $\mu = \frac{1}{2} \sum_{jr} (k_{jr} + \sum_s \omega_{jrs})$, and $m_s = \sum_j k_{js}$ and $\delta(g_{is}, g_{jr})$ equals 1 if node i of layer s belongs to the same module as node j of layer r. γ_s is the resolution parameter for layer s, and ω_{jrs} represents the interlayer connectivity of node j between layers r and s. Here, we consider the same γ_s for all layers and $\omega_{jrs} \neq 0$ only if r and s are consecutive layers; furthermore, all non-zero entries of ω_{jrs} are equal.

http://netwiki.amath.unc.edu/GenLouvain/GenLouvain

Regional probability of belonging to the thalamic module

Regional probability of belonging to the thalamic module

We computed the regional probability of belonging to the same module as the bilateral thalamus ROI:

$$P_i = \frac{\#\left\{t : M_i(t) = C(t)\right\}}{T}$$

Here P_i is the probability of finding the i-th region in the same module as the thalamus, $M_i(t)$is the module assignment of region i at time t, $C(t)$is the module assignment of the thalamic regions at time t, and $T$is the total time is the number of time points considered for the analysis (in our case, 120).